

SAND78-2101C

PLASMA-SPRAYED COATINGS FOR FUSION REACTOR APPLICATIONS*

A. W. Mullendore, D. M. Mattox, J. B. Whitley and D. J. Sharp
 Sandia Laboratories**
 Albuquerque, New Mexico 87185

ABSTRACT

A series of plasma-sprayed coatings has been given a preliminary evaluation to assess the potential of this class of materials in fusion reactor applications. TiC, TiB₂, Be and VBe₁₂ coatings on copper and stainless steel were tested for coating adherence, ion erosion resistance and susceptibility to arc erosion. The coatings, in general, display a good resistance to thermal shock failure. The TiC and TiB₂ coatings exhibit favorable ion erosion characteristics and the resistance of the coatings to arc erosion was, in general, superior to that of stainless steel.

NOTICE
 This report was prepared as an account of work sponsored by the United States Government. Neither the United States nor the United States Department of Energy, nor any of its employees, nor any of the contractors, subcontractors, or their employees, make any warranty, express or implied, or assumes any legal liability or responsibility for the accuracy, completeness or usefulness of any information, apparatus, product or process disclosed, or represents that its use would not infringe privately owned rights.

MASTER

*This work is supported by the Division of Materials and Radiation Effects Branch of the Office of Fusion Energy, U. S. Department of Energy (DOE), under Contract DE-AC04-76-DP00789.

**A U. S. DOE facility.

INTRODUCTION

The internal surfaces of a tokamak fusion reactor control the impurity injection and gas recycling into the fusion plasma. Coating of these surfaces provides design flexibility for achieving the temperatures, ion densities and containment times necessary for useful fusion reactions to take place.¹ The requirements on materials in close proximity to the plasma in a fusion reactor include resistance to: 1) erosion by chemical or physical processes and, 2) failure from rapid temperature changes, and severe thermal gradients.

A variety of coating species and methods of application (chemical vapor deposition, plasma spraying and chemical conversion) are being evaluated in our laboratory.¹ Plasma spraying has the advantage of versatility - virtually, any material with a melting transition can be applied to a suitable substrate. Thus, refractory, erosion resistant and preferably low atomic number materials can be selected for coating a substrate with the appropriate bulk mechanical and thermal properties. The coatings can possess quite good thermal shock resistance, perhaps by virtue of their distention. They can be applied economically and are potentially renewable, even in situ. Some features of the coatings may be less desirable. The porosity, high surface area and frangibility of some coatings may result in undesirable gas adsorption and recycle characteristics and in enhanced erosion.

Our evaluation of plasma-sprayed coatings has started with TiC, TiB₂, Be and VBe₁₂ coatings on copper and stainless steel

substrates. They have been tested for adhesion, low energy ion erosion and arc erosion. The potential use of hot isostatic pressing for densification or bond improvement has also been examined. These results are intended to guide the subsequent phases of material selection and further development of promising candidate materials.

EXPERIMENTAL

Sample preparation* was accomplished by numerous automated spraying passes onto 1.27 and 2.54 cm diameter by 0.05 and 0.64 cm thick substrates mounted on a rotating cylindrical mandrel. On copper substrates an adherence layer (~0.002 cm thick) of copper was applied by plasma spraying prior to application of the 0.013 to 0.020 cm thick coating. Table 1 summarizes the results of emission spectroscopic analysis of impurities and mercury porosimetry analysis of pore volume and surface area. X-ray diffraction was used to confirm the nominal stoichiometry of the coatings and showed no evidence of other phases.

Coating adhesion was initially assessed by 180° bend tests of 0.05 cm thick substrate samples about a 1.27 cm diameter rod. Optical inspection and metallographic sectioning of bend samples were used to detect damage. All coatings except TiB_2 exhibited a dense pattern of cracks through the coating throughout the bend area but none exhibited surface spall or extensive layer separation. With TiB_2 , the cracking was not observable because of a powdery (not well fused) character of the coating.

*Plasma-spraying, chemical analysis, mercury porosimetry and bend testing were done at the Y-12 Division of Union Carbide Corp. at Oak Ridge, TN.

Edge delamination was observed for VBe₁₂ on stainless steel. Layer cracking was evident for VBe₁₂ on Cu and stainless steel, TiC on Cu and stainless and Be on Cu. None of these was thought to eliminate any candidate from further consideration.

Adhesion under conditions of pulsed energy input of high intensity and short duration, as in the fusion reactor environment, was evaluated in the electron beam test apparatus described in Ref. 2. The 0.64 cm thick substrate samples resting on a water cooled copper hearth were subjected to repeated 0.7 sec. pulses of 2 kW/cm² energy density until failure or for 50 cycles without failure.

Table 1. Plasma Spraying Analyses*

	TiC	TiB ₂	Be	VBe ₁₂
Total impurities - ppm	3050	2470	940	800
Surface area - M ² /g	0.59	0.65	4.75	1.37
cm ² /cm ² †	340	302	1070	500
Porosity - %	24.8	33.4	29.7	19.3
Average pore diam. - μm	4.9	4.7	4.1	10.4
Porosity <10μm - %	90.9	94.7	93.0	74.1
Thickness - cm	0.016	0.016	0.017	0.019

*Average for 0.64 cm thick Cu and SS substrates.

†Coating surface area per unit substrate area.

An initial assessment was made of the potential of hot isostatic pressing for improving the coating/substrate bond or for coating densification. Two stacks of 2.54 cm diameter x 0.05 cm thick wafers of all coating-substrate combinations were prepared with thin spacers of Al₂O₃ separating each sample.

They were encased in close fitting thin walled stainless steel cans, evacuated and closed by electron beam welding and then subjected to hot isostatic pressing for two hours at 943 K and 207 MPa.

Low energy ion erosion yields, at normal incidence, were determined using a Kaufman ion source.^{2,3} Erosion yields by mixed hydrogenic species (H^+ , H_2^+ , H_3^+) and xenon were determined for 250 eV, 500 eV and 1000 eV ions at a dose rate of about 0.5 ma/cm². Erosion rates of atoms per ion were determined by weight loss methods.

The experimental configuration used to study the relative arcing behavior of the coated samples is shown in Figure 1. The samples are immersed in a low density ($\sim 10^{12}$ cm⁻³) low energy (3-4 eV) DC plasma. Small unipolar arcs form on the cathodic surfaces under unstable discharge conditions. A negative bias and a capacitor energy storage system connected to the sample allowed the low energy unipolar arcs to develop into high energy (80 Joule) plasma arcs. A "catcher" plate was positioned to one side to collect ejected materials.

RESULTS AND DISCUSSION

Adhesion Testing

The aim of this screening test was to observe any tendency for coating failure (cracking, spalling, melt, etc.) under constant conditions of pulsed electron beam power input. The number of cycles to failure and the failure type were the bases of comparison. Table 2 shows these results. TiB_2 and TiC

coatings on Cu survived 50 cycles of 0.7 sec. duration and 7 seconds between pulses with no disruption of the coating.

Table 2. Electron Beam Adhesion Testing

Material	Cycles at 21 Sec Interval	Cycles at 7 Sec Interval	Total	Failure Mode
TiB ₂ /Cu	5	45	50	No Failure (2 hot spots)
TiB ₂ /SS	5	5	10	Alloying and Substrate Melt
TiC/Cu	5	45	50	No Failure (2 hot spots)
TiC/SS	5	5	10	Alloying and Substrate Melt
VBe ₁₂ /Cu	5	45	50	Alloying and Substrate Melt
VBe ₁₂ /SS	2	--	2	Alloying and Substrate Melt
Be/Cu	5	17	22	Alloying and Substrate Melt
Be/SS	5	20	25	Alloying and Substrate Melt

There was visual evidence of local hot spots during the testing. These did not produce failure but appear to have promoted alloying and isolated substrate melting spots. On stainless steel, failures occurred after 10 cycles for both TiC and TiB₂ and were due to substrate melting. The coatings were still intact but had a lighter, more silvery color in the substrate melt area. VBe₁₂ on copper was also subjected to 50 cycles but interdiffusion of coating and substrate was evident from a change in color of the coating to a copper hue and the appearance of some sub-surface melting. On stainless steel, the same process led to substrate melting after two cycles. Beryllium failed by

substrate alloying and melt at 22 and 25 pulses on Cu and stainless substrates respectively. Thus, in all of the testing, there was no evidence of coating spall and the only sign of localized deadhesion was the appearance of hot spots which would suggest an interruption of the thermal conduction path. The stainless steel substrate, in general, produced earlier failures because of its lower conductivity and resultant higher surface temperatures.

Hot Isostatic Pressing

The conditions of the hot isostatic pressing (943 K, 207 MPa) were dictated primarily by the substrates used and, in particular, by the copper substrate. It was not expected that any densification of the TiB_2 , TiC or VBe_{12} coatings would occur and this was born out by the metallographic examination of pressed samples. Three distinct effects were observed. First, copper intrusion into the pores of all coatings over a distance of 0.02 mm occurred and is expected to improve bond strength and to moderate differential thermal expansion effects. Secondly, excellent densification of the Be coating was observed. Thirdly, interdiffusion and intermetallic formation were observed with Be-Cu and VBe_{12} -Cu samples. Figure 2 illustrates all three effects. The as-sprayed structure is shown at the left and the hot pressed structure on the right shows the densified Be (Zone A), the region of Cu intrusion and interaction (Zone C) and the interdiffusion zones (B and D). Electron microprobe analysis for copper has indicated the presence of four Cu-Be phases in the regions of interaction whose composition corresponds to $CuBe$, Cu_2Be_3 , $CuBe_4$ and $CuBe_{13}$.

Low Energy Ion Erosion Yields

Table 3 gives the relative atomic erosion yields of the plasma sprayed materials under the conditions indicated. The data indicates that the erosion rate by high Z (Xe = 131) ions can be a factor of 100 or more greater than the erosion rate by hydrogenic ions.

Table 3

EROSION YIELD (ATOMS/ION)
PLASMA SPRAYED MATERIALS

	HYDROGEN		XENON		
	Dose	Energy	Dose	Energy	Dose
	2.2×10^{21}	250 eV	1.4×10^{21}	500 eV	2.1×10^{21}
			7.6×10^{19}	250 eV	2.1×10^{19}
TiB ₂	0.0009	0.006	0.0096	0.34	1.12
TiC	0.0008	0.005	0.008	0.07	0.60
VBe ₁₂	0.004	0.008	0.016	0.11	0.81
Be	0.006	0.012	0.016	0.09	0.60

Approximately 5 micrometers of material was removed by the hydrogen and xenon erosion at 1000 eV. The resulting erosion morphologies show that, except for the beryllium, erosion smoothed the as-deposited surface. For beryllium, hydrogen erosion produced a cone morphology on the surface⁴ while xenon did not. The cone formation is probably due to carbon contamination of the surface during erosion.

Arc Erosion Testing

All materials tested in the plasma arcing chamber produced high energy arcs. Prior to applying the negative bias to the samples, the surfaces showed regions of small microarcs. With

repetitive arcing, the arcing rate was found to decrease with the surfaces ceasing to initiate arcs after a period of time. This conditioning process seemed to have two primary effects, mainly the removal of sharp protrusions and other highly arc prone areas from the surface and secondly, the removal of oxides and other surface layers.

Optical micrographs of several arced surfaces are shown in Figure 3. In general, the arc tracks in metals consist of a region of adjoining craters of melted material. In materials such as copper or stainless steel, the melt regions are large (~0.25 mm diameter) and the catcher plates show that a large fraction of the eroded materials was ejected as liquid droplets of up to 10 μ m diameter. For refractory coatings such as TiB₂, the surface melting is generally less intense and the droplets are found to be much smaller.

The surfaces of the plasma sprayed coatings are quite rough and porous and large chunks of unmelted eroded materials have been found on the catcher plates. In the case of TiB₂ on Cu, arcing resulted in the melting and local spall of the coating exposing the underlying substrate material. The other coatings did not exhibit this failure mode. In general, the plasma sprayed coatings examined in this study showed less susceptibility for arcing than bulk stainless steel.

CONCLUSIONS

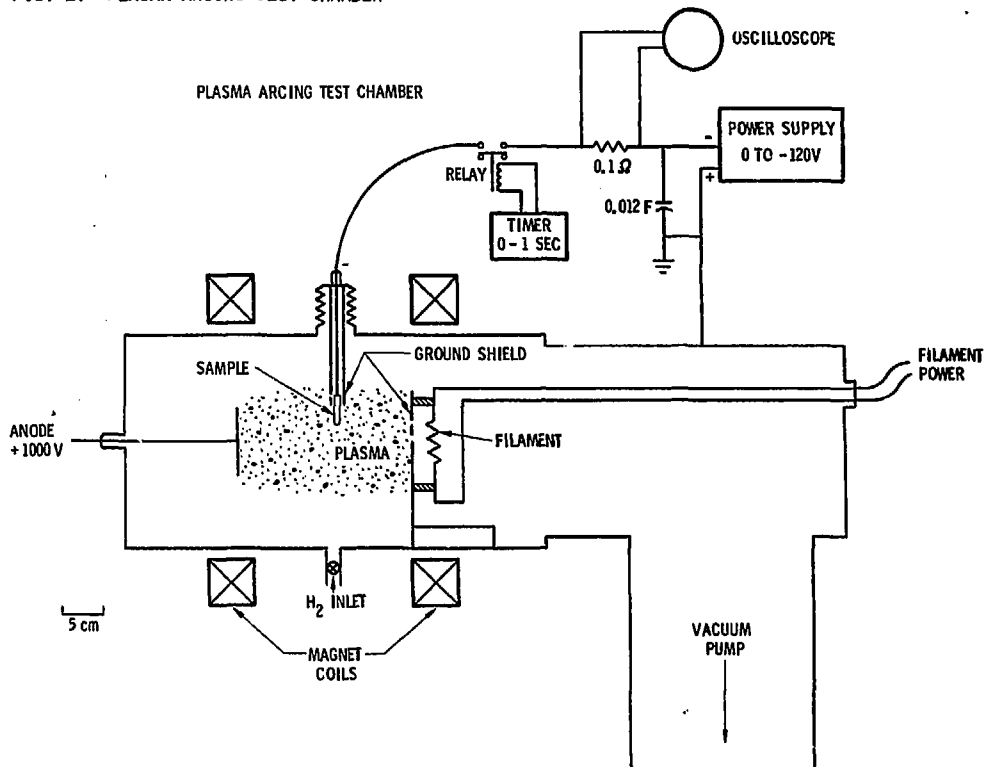
Initial evaluations have been made of the potential of plasma sprayed coatings for fusion reactor applications.

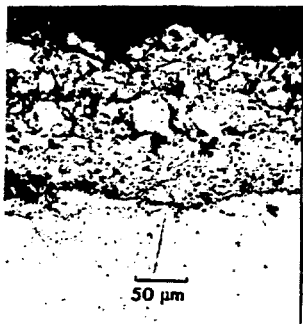
The results of adhesion testing, hot isostatic pressing experiments, ion erosion studies and examination of the susceptibility to arc erosion have indicated that, in general, quite satisfactory performance of this class of materials can be obtained.

REFERENCES

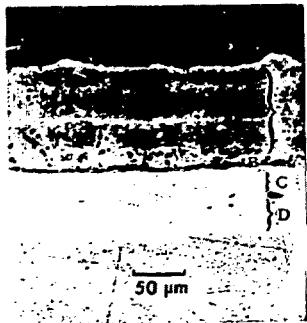
1. D. M. Mattox, "Coatings for Fusion Reactor Applications," presented to the International Metallurgical Coating Conference, San Diego, CA, April 23-27, 1979. To be published in proceedings issue of Thin Solid Films.
2. D. M. Mattox, A. W. Mullendore, H. O. Pierson and D. J. Sharp, "Low Z Coatings for Fusion Reactor Applications," presented to the First Topical Meeting on Fusion Reactor Materials, Bal Harbour, FL, 1979. To be published in proceedings issue of J. Nucl. Mat.
3. D. M. Mattox and D. J. Sharp, "Low Energy Hydrogen Ion Erosion Yields as Determined with a Kaufman Ion Source," Sandia Labs Report SAND78-1029 (Oct. 1978).
4. D. M. Mattox and D. J. Sharp, "Influence of Surface Morphology on the Low Energy Hydrogen Ion Erosion Yields of Beryllium," J. Nucl. Mat. 80, 115 (1979).

FIG. 1. PLASMA ARCING TEST CHAMBER





a.



b.

Fig. 2. Optical micrographs of plasma-sprayed beryllium on copper: a. as-sprayed; b. after hot isostatic pressing.

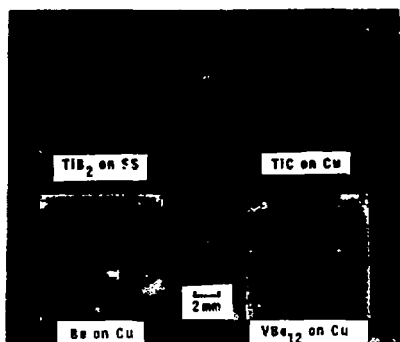


Fig. 3. Arc tracks on plasma sprayed coatings.